arXiv:0912.5282v1 [quant-ph] 29 Dec 2009

Dissipative Dynamics with Trapping in Dimers

Oliver Mülken, Lothar Mühlbacher, Tobias Schmid, and Alexander Blumen
Physikalisches Institut, Universität Freiburg, Hermann-Herder-Straße 3, 79104 Freiburg, Germany
(Dated: February 4, 2022)

The trapping of excitations in systems coupled to an environment allows to study the quantum to classical crossover by different means. We show how to combine the phenomenological description by a non-hermitian Liouville-von Neumann Equation (LvNE) approach with the numerically exact path integral Monte-Carlo (PIMC) method, and exemplify our results for a system of two coupled two-level systems. By varying the strength of the coupling to the environment we are able to estimate the parameter range in which the LvNE approach yields satisfactory results. Moreover, by matching the PIMC results with the LvNE calculations we have a powerful tool to extrapolate the numerically exact PIMC method to long times.

PACS numbers: 05.60.Gg, 05.60.Cd, 71.35.-y

I. INTRODUCTION

Recent years have seen growing interest in coherent energy transfer. For instance, it has been pointed out that photosynthesis might benefit from quantum mechanical features of the transfer of excitations created by the incoming solar energy [1]. A series of papers has modelled coherent dynamics in the light-harvesting system of the photosynthetic unit showing that the coupling to an environment does not necessarily destroy all coherent features – even at room temperature – but also can support the coherent transfer of excitations [2]. The majority of these studies use the Lindblad form of the Liouville von Neumann equation (LvNE) for the reduced density operator of the system where the environmental degrees of freedom have been traced out [3]. However, this approach is only valid in a limited parameter range of the coupling to the environment.

In contrast, rapid experimental advances allow to manipulate and control ultra-cold atoms to a large extent. This offers the possibility to study coherent transport and the effect of environment changes (e.g., an increase in the temperature). An ideal system to study the dynamics of excitations are (frozen) Rydberg gases [4], whose atoms can have complex spatial arrangements, for which the coherent dynamics can be efficiently modelled by continuous-time quantum walks [5].

Moreover, it is possible to adjust the properties of specific ("special") single atoms such that the excitation gets to be absorbed at these atoms [6, 7]. In this way they mimic the reaction center (RC) of photosynthesis, where the excitation gets trapped and further processed. Both systems can be viewed as being donor-acceptor units, where the excitation is created at the donor ("normal" Rydberg atoms, light-harvesting complex) and gets absorbed at the acceptor ("special" Rydberg atoms, RC). The decay of the excitation at the acceptor allows to globally monitor the transport dynamics.

While the LvNE approach allows for a phenomenological modelling, other methods treat the system and the coupling to the environment in a microscopic manner. Our method of choice is the path integral Monte Carlo (PIMC) technique, see, e.g., [8, 15], which can be applied for arbitrary system-environment coupling strengths. However, unlike the LvNE approach, the real-time PIMC method is plagued by the notorious dynamical sign problem [14], which significantly limits the time scales accessible to PIMC simulations. However, by combining the LvNE and the PIMC methods we are able to study excitation dynamics and trapping over large timescales and improve the numerical accuracy of our results.

Our model system is a dimer, represented by two coupled two-level systems (TLS), one of which acting as trap, the dimer being coupled to the environment. By assuming not too strong couplings to the environment and a single initial excitation of one of the TLS, one can map the two TLS onto a single TLS, if, without the trap, the probability of finding the excitation in the system is conserved [9]. We note that various systems with, e.g., radial symmetry and a trap in the center can effectively be mapped onto the dimer if initially the excitation is homogeneously distributed over the periphery [10].

II. COHERENT EXCITON TRAPPING

In general, we consider the Hamiltonian of a network of N nodes, where each node represents a single two-level system. Let $\boldsymbol{H}_0$ be the Hamiltonian without traps. The accessible Hilbert space is completely characterized by the basis states $|j\rangle$ which are associated with excitations localized at the nodes $j = 1, \ldots, N$. Within a phenomenological approach, the Hamiltonian, which incorporates trapping of excitations at the nodes $m \in \mathcal{M}$, $\mathcal{M} \subset \{1, \ldots, N\}$, is given by $\boldsymbol{H} \equiv \boldsymbol{H}_0 - i\boldsymbol{\Gamma}$, where $i\boldsymbol{\Gamma} \equiv i\Gamma \sum_m |m\rangle\langle m|$ is the trapping operator, see Ref. [6] for details. As a result, $\boldsymbol{H}$ is non-hermitian and has N complex eigenvalues, $E_l = \epsilon_l - i\gamma_l$ ($l = 1, \ldots, N$) where $\gamma_l > 0$, and N right and N left eigenstates, denoted by $|\Phi_l\rangle$ and $\langle\tilde{\Phi}_l|$, respectively. The transition probability from node j to node k is then given by

$$\pi_{k,j}(t) = \left| \sum_l \exp(-\gamma_l t) \exp(-i\epsilon_l t) \langle k|\Phi_l\rangle\langle\tilde{\Phi}_l|j\rangle \right|^2, \quad (1)$$

so that the negative imaginary parts γ_l of E_l determine the temporal decay. The mean survival probability $\Pi(t)$ of an excitation in the presence of M trap nodes is a global property of the network and is defined as

$$\Pi(t) \equiv \frac{1}{N-M} \sum_{j\neq m} \sum_{k\neq m} \pi_{k,j}(t), \quad (2)$$

i.e., $\Pi(t)$ is the average of $\pi_{kj}(t)$ over all initial nodes j and all final nodes k, neither of them being a trap node.

A. Liouville-von Neumann equation

The Schrödinger equation can be recast into the Liouville-von Neumann equation (LvNE) when considering the density operator $\boldsymbol{\rho}$. For Hermitian Hamiltonians $\boldsymbol{H}_0$ one has $\dot{\boldsymbol{\rho}} = -i\big[\boldsymbol{H}_0, \boldsymbol{\rho}\big]$, where $[\cdot,\cdot]$ is the commutator. Now, for the non-hermitian Hamiltonian $\boldsymbol{H}$ one obtains

$$\dot{\boldsymbol{\rho}} = -i\big[\boldsymbol{H}_0, \boldsymbol{\rho}\big] - \big\{\boldsymbol{\Gamma}, \boldsymbol{\rho}\big\}, \tag{3}$$

where $\{\cdot,\cdot\}$ is the anti-commutator.

Introducing the coupling to the environment naturally complicates the situation. However, under certain conditions one can employ the so-called Lindblad form of the LvNE, where the Lindblad operators specify the coupling [3]. Consider now Lindblad operators which can be written as $\sqrt{\lambda_j}\boldsymbol{L}_j$, where λ_j is a fixed decay rate. Assuming all rates to be equal, $\lambda_j \equiv \lambda$ for all j, the LvNE reads

$$\dot{\boldsymbol{\rho}} = -i\big[\boldsymbol{H}_0, \boldsymbol{\rho}\big] - \big\{\boldsymbol{\Gamma}, \boldsymbol{\rho}\big\} - 2\lambda \sum_j \Big(\boldsymbol{\rho} - \langle j|\boldsymbol{\rho}|j\rangle\Big)\boldsymbol{L}_j. \tag{4}$$

The rate λ can be estimated from the spectral density $J(\omega)$ describing the environment within the Caldeira-Leggett model [12] at a given temperature T. Taking $J(\omega) = 2\pi\alpha\omega\exp(-\omega/\omega_c)$ and using the Markov approximation one arrives at $\lambda = \pi\alpha k_B T$ [3]. One has to bear in mind that Eq. (4) is an approximation with a limited range of validity: For a very large coupling strength λ, Eq. (4) leads to the quantum Zeno limit rather than to a classical master/rate equation. In the following we will consider Lindblad operators which are given by projection operators of the type $\boldsymbol{L}_j \equiv |j\rangle\langle j|$ [3].

III. DIMERS WITH TRAPS

In the sequel we will consider a dimer which is coupled to an external bath. This system allows to solve Eq. (4) analytically and, moreover, to compare the approximate LvNE results to the numerically exact PIMC calculations. The Hamiltonian of the dimer without any coupling to the surroundings can be expressed through the Pauli matrices $\boldsymbol{\sigma}_z$ and $\boldsymbol{\sigma}_x$,

$$\boldsymbol{H} = E\,\mathbf{1} - V\boldsymbol{\sigma}_x + i\frac{\Gamma}{2}(\mathbf{1} - \boldsymbol{\sigma}_z)\,, \tag{5}$$

where E is the onsite energy, which we choose to be the same for both nodes, and V is the coupling between the two nodes. It is easily verified that the eigenvalues are

$$E_\pm = E \pm Ve^{\pm i\phi} = E \pm \sqrt{V^2 - \Gamma^2/4} - i\Gamma/2, \tag{6}$$

where $\phi = \arcsin(\Gamma/2V)$. For $\Gamma \to 0$ ($\phi \to 0$) this yields the correct eigenvalues $E \pm V$ of $\boldsymbol{H}_0$. Note that for $\Gamma \leq 2V$ the negative imaginary part of $E_\pm$ is identical for both eigenvalues, i.e., $\gamma_+ = \gamma_- = \Gamma/2$. The bi-orthonormalized eigenstates of $\boldsymbol{H}$ are of the form

$$|\Phi_\pm\rangle \equiv \frac{1}{\sqrt{2\cos\phi}}\begin{pmatrix} e^{\pm i\phi/2} \\ \pm e^{\mp i\phi/2}\end{pmatrix} \tag{7}$$

and

$$|\tilde{\Phi}_\pm\rangle \equiv \frac{1}{\sqrt{2\cos\phi}}\begin{pmatrix} e^{\mp i\phi/2} \\ \pm e^{\pm i\phi/2}\end{pmatrix}, \tag{8}$$

where the phases ϕ depend on Γ such that in the limit $\Gamma \to 0$ one recovers the eigenstates of $\boldsymbol{H}_0$.

We note, however, that finding the bi-orthonormal basis set is not necessary for the following calculations. One just has to require that the basis sets of $\boldsymbol{H}$ and $\boldsymbol{H}^\dagger$ are orthonormal, respectively. In this way one diagonalizes $\boldsymbol{H}$ and $\boldsymbol{H}^\dagger$ separately, which in the end leads to the same eigenvalues and eigenstates as the approach described above.

When the coupling to the environment vanishes ($\lambda \to 0$) one obtains the survival probability directly from the eigenstates and eigenvalues of $\boldsymbol{H}$. For $\Gamma \leq 2V$ one has

$$\Pi(t) = e^{-\Gamma t}\frac{\cos^2(\phi + tV\cos\phi)}{\cos^2\phi} \quad (\text{for } \lambda = 0). \tag{9}$$

We note that for values $\Gamma > 2V$ the dimer is overdamped.

When considering the dimer without traps ($\Gamma = 0$) but coupled to the environment, Eq. (4) simplifies and, from the solution for $\boldsymbol{\rho}$, one obtains the transition probabilities

$$\pi^{(0)}_{1,1}(t) = \frac{1}{2} \;+\; \frac{e^{-\lambda t}}{2}\left[\frac{\lambda\sin\left(t\sqrt{4V^2-\lambda^2}\right)}{\sqrt{4V^2-\lambda^2}} + \cos\left(t\sqrt{4V^2-\lambda^2}\right)\right] \quad (\text{for } \Gamma = 0) \tag{10}$$

and $\pi^{(0)}_{2,1}(t) = 1 - \pi^{(0)}_{1,1}(t)$. For $\lambda \to 0$ one recovers the simple oscillatory behavior of the transition probabilities [namely, $\lim_{\lambda\to 0}\pi^{(0)}_{1,1}(t) = \cos^2(Vt)$]. For $\lambda > 0$, i.e., with coupling to the surroundings, the transition probabilities still show oscillations superimposed on an exponential decay in time which tends to the classical equipartition value of $1/2$.

In order to combine the results of Eq. (9) – we will only focus on values $\Gamma < 2V$ at this stage – and Eq. (10), we expand in both equations all terms except the exponentials to first order in Γ and λ, respectively. Note that for Eq. (9) we obtain a product of $\exp(-\Gamma t)$ and $\cos^2 Vt$, which is the simple oscillatory behavior of the dimer without trap. Now, the coupling to the environment affects all transitions but still conserves probabilities. Therefore, we replace the term $\cos^2 Vt$ by the expansion of Eq. (10), by which we obtain

$$\begin{aligned}\Pi(t) \;&\approx\; e^{-\Gamma t}\pi^{(0)}_{1,1}(t) \\ &\approx\; e^{-\Gamma t}\Big[\frac{1}{2} + \frac{e^{-\lambda t}}{2}\Big(\cos 2Vt + \frac{\lambda}{2V}\sin 2Vt\Big)\Big]\end{aligned} \tag{11}$$

A. PIMC

In order to corroborate our results we will compare the phenomenological LvNE approach described above to the numerically exact PIMC calculations based on a microscopic modelling of the dissipative environment. This allows to judge for which parameter range the approximation by Eq. (4) delivers satisfactory results.

When coupling the dimer to a bath, the total Hamiltonian reads $\boldsymbol{H}_{\rm tot} = \boldsymbol{H} + \boldsymbol{H}_{\rm I} + \boldsymbol{H}_{\rm B}$, where the dimer-bath coupling and bath are described in the framework of the Caldeira-Leggett model [12],

$$\boldsymbol{H}_{\rm I} + \boldsymbol{H}_{\rm B} = -\boldsymbol{\sigma}_z \sum_\kappa c_\kappa \boldsymbol{X}_\kappa + \sum_\kappa \left(\frac{\boldsymbol{P}_\kappa^2}{2m_\kappa} + \frac{1}{2} m_\kappa \omega_\kappa^2 \boldsymbol{X}_\kappa^2 \right) . \tag{12}$$

Here, $\boldsymbol{P}_\kappa$ and $\boldsymbol{X}_\kappa$ are the momentum and position operators of the bath degrees of freedom, respectively, while m_κ and ω_κ denote their mass and frequency. The counter term, which prevents a renormalization of the free dimer's energy levels due to the environmental coupling [11], is absent in Eq. (12) since it reduces to a physically irrelevant constant in the case of a two-level system. After tracing out the environmental degrees of freedom, the onsite population of node $|n\rangle$ becomes

$$\pi_{n,1}(t) = \oint \mathcal{D}\tilde{\sigma}\, \delta_{\tilde{\sigma}(t),n} \exp\left\{ \frac{i}{\hbar} S[\tilde{\sigma}] - \Phi[\tilde{\sigma}] \right\} , \tag{13}$$

where $\tilde{\sigma}$ denotes a closed quantum path in terms of the eigenstates of $\boldsymbol{\sigma}_z$ with $\tilde{\sigma}(0) = -1$ (referring to the initial preparation in node $|1\rangle$), and $S[\tilde{\sigma}]$ is the action of the free dimer. The influence of the environment is summarized in the Feynman-Vernon influence functional $\Phi[\sigma]$ [13], which is completely determined by the environment's spectral density,

$$J(\omega) = \frac{\pi}{2\hbar} \sum_\alpha \frac{c_\kappa^2}{m_\kappa \omega_\kappa} \delta(\omega - \omega_\kappa) ; \tag{14}$$

for further details, we refer to Ref. [11].

As the exact dynamics Eq. (13) can not be calculated analytically, one has to resort to a numerical evaluation of the path integral. Here, the PIMC method has proven to be a promising approach to obtain numerically exact results even in regions of parameter space where approximative methods fail (for details, see e.g. Refs. [8, 15]). In our case it is straightforward to adopt the approach presented in Ref. [15] once the free dimer's forward and backward propagators, which define $S[\tilde{\sigma}]$, are expressed according to

$$\begin{aligned} \langle n| \exp(-i\boldsymbol{H}t/\hbar)|n'\rangle &= \sum_{\sigma=\pm} \langle n|\Phi_\sigma\rangle\langle\tilde{\Phi}_\sigma|n'\rangle\, e^{-iE_\sigma t/\hbar} , \\ \langle n'| \exp(i\boldsymbol{H}^\dagger t/\hbar)|n\rangle &= \sum_{\sigma=\pm} \langle n'|\Phi_\sigma\rangle\langle\tilde{\Phi}_\sigma|n\rangle\, e^{iE_\sigma^* t/\hbar} , \end{aligned} \tag{15}$$

which, even for $\Gamma \neq 0$, are complex conjugate to each other.

IV. COMPARISON OF LVNE TO PIMC

Figure 1 compares the survival probabilities of a dissipative dimer obtained from the approximative LvNE approach to the numerically exact PIMC calculations for a bath with ohmic spectral density (14) with exponential cutoff, $J(\omega) = 2\pi\alpha\omega e^{-\omega/\omega_c}$. Here, the onsite energies E and the coupling elements V have been taken to be equal, $E = V = 1$, while the temperature is fixed to $k_B T = V$, and we set $\omega_c = 5V$.

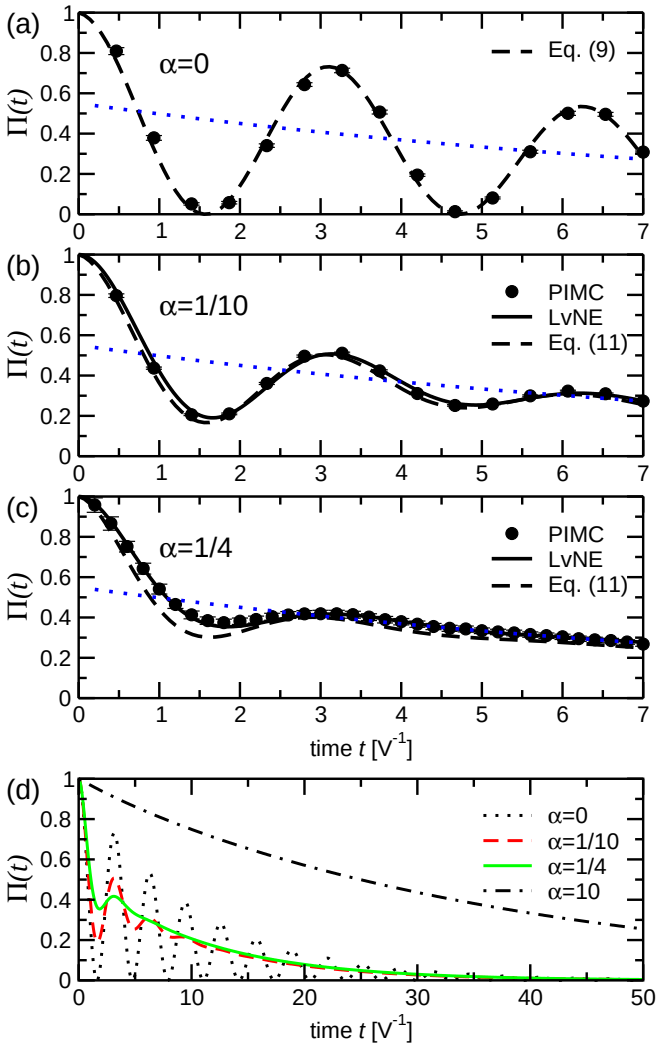


FIG. 1: (Color online) PIMC results (circles) for a dimer with $\Gamma = 0.1$ and different system-bath couplings $\alpha = \lambda/\pi$: (a) $\alpha = 0$, (b) $\alpha = 1/10$, and (c) $\alpha = 1/4$. The solid lines represent the numerical solution of the LvNE equation, the dashed lines show the corresponding analytical results obtained from Eq. (9) for $\alpha = \lambda = 0$ and from Eq. (11) for $\alpha = 1/10$ and $\alpha = 1/4$. The dotted blue line shows the long time limit $\Pi(t) \sim \exp(-\Gamma t)$. Panel (d) shows the corresponding long-time behavior of the numerical LvNE solution for the three different values of α and additionally the behavior for large couplings $\alpha = 10$.

For small trapping strength ($\Gamma = 0.1$) and vanishing coupling to the environment ($\alpha = 0$), Fig. 1(a), the PIMC calculations coincide with the result of Eq. (9). A moderate increase

of the coupling ($\alpha = 1/10$), Fig. 1(b), still leads for Eqs. (4) (solid lines) and (11) (dashed lines) to results which are in excellent agreement with the findings of the PIMC calculations (symbols). When increasing the coupling further to $\alpha = 1/4$, Fig. 1(c), however, the approximate solution, Eq. (11), begins to deviate from the LvNE and the PIMC calculations, which are still in very good agreement.

As the numerical effort of real-time PIMC simulations grows exponentially with time, they can cover only short-to-intermediate timescales. However, the agreement between the LvNE and the PIMC calculations in the weak coupling regime allows to compensate for this shortcoming, by using at longer times the LvNE results, see Fig. 1(d).

As mentioned earlier, strong couplings λ in the LvNE lead to the Zeno limit, and therefore disagree with the large-coupling/high-temperature behavior of the PIMC formalism. Figure 1(d) shows $\Pi(t)$ for $\alpha = 10$ (dashed-dotted line), which clearly deviates from the long-time behavior of the curves for small α-values. This corroborates the fact that the LvNE in the Lindblad form only yields the correct long-time behavior for rather weak couplings to the environment.

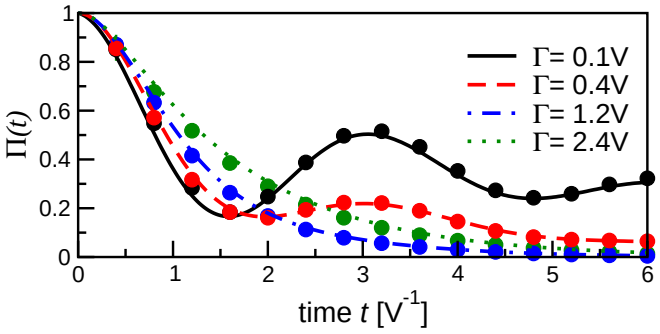


FIG. 2: (Color online) Dimer with $\alpha = 1/10$ and different trapping strengths Γ. The lines represent the numerical solution of the LvNE and the symbols show the corresponding PIMC results.

For $\alpha = 1/10$ and varying Γ, Fig. 2 compares $\Pi(t)$ obtained from the numerical solution of the LvNE to the results of the corresponding PIMC calculations. The trap is part of the system, i.e., it directly enters the Hamiltonian $\boldsymbol{H}$. Therefore, unlike a change in α, a change in Γ leads to no significant differences for $\Pi(t)$ obtained from the two methods. Nevertheless, varying the trapping strength has strong implications for the survival probability: At short times ($t < 2$) the survival probability $\Pi(t)$ is smaller for smaller Γ. At larger times the decay is very pronounced for larger Γ-values; smaller Γ-values do not dampen the oscillations which are superimposed on the decay. This effect will be weakened when increasing the coupling to the environment.

V. THE INCOHERENT CASE

Finally, in the limit of very strong coupling to the environment, all coherences will be quickly destroyed and the resulting transport becomes purely incoherent. The dynamics is governed by a master equation whose transfer matrix is

$$\boldsymbol{T} = \begin{pmatrix} \tilde{E} & -\tilde{V} \\ -\tilde{V} & \tilde{E}+\tilde{\Gamma} \end{pmatrix}, \tag{16}$$

One obtains the parameters $\tilde{E}$, $\tilde{V}$, and $\tilde{\Gamma}$ by fitting to the PIMC calculations at large temperatures. In principle one can obtain the transfer rates $\tilde{V}$ from a golden rule approach [16]. The matrix $\boldsymbol{T}$ has purely real eigenvalues,

$$\lambda_\pm = \tilde{E} \pm \tilde{V} e^{\mp\psi} = \tilde{E} + \tilde{\Gamma}/2 \pm \sqrt{\tilde{V}^2 + \tilde{\Gamma}^2/4}, \tag{17}$$

Similar to the coherent case, the eigenstates of $\boldsymbol{T}$ read

$$|\Psi_\pm\rangle \equiv \frac{1}{\sqrt{2\cosh\psi}} \begin{pmatrix} e^{\pm\psi/2} \\ \pm e^{\mp\psi/2} \end{pmatrix} \tag{18}$$

where $\psi = \mathrm{arcsinh}(\tilde{\Gamma}/2\tilde{V})$. Now, the classical survival probability is readily obtained as

$$P(t) = p_{1,1}(t) = e^{-t(\tilde{E}+\tilde{\Gamma}/2)} \frac{\cosh\left(\psi + t\tilde{V}\cosh\psi\right)}{\cosh\psi}, \tag{19}$$

which for not too small t gives rise to a simple exponential decay with exponent λ_+. Taking $\tilde{E} = \tilde{V}$ and $\tilde{\Gamma} \ll 1$ one obtains $P(t) \sim e^{-t\tilde{\Gamma}/2}$, which is independent of $\tilde{E}$ and $\tilde{V}$. We note the difference in the overall exponential decay of the LvNE which was proportional to $\exp(-\Gamma t)$. Comparing this to the PIMC results for strong couplings α, we obtain $\tilde{\Gamma} = 2\Gamma$.

VI. CONCLUSIONS

We have studied the trapping of excitations in dimers which are coupled to a dissipative environment. By using the (approximative) Lindblad form of the LvNE on one hand and the (numerically exact) PIMC calculations on the other, we were able to specify the range of coupling parameters in which both methods agree with each other. Moreover, matching the two approaches by appropriately adjusting the coupling parameter α in the LvNE allows to extrapolate the short-to-intermediate-time PIMC result to – in principle – arbitrary long times. Since PIMC is numerically exact, the combination with the LvNE is ideal for also studying large systems at long times for a broad range of couplings.

Acknowledgements

Support from the Deutsche Forschungsgemeinschaft (DFG) and the Fonds der Chemischen Industrie is gratefully acknowledged. LM acknowledges computational support from the Black Forest Grid of the computing center of the university of Freiburg.

[1] G. R. Fleming and G. D. Scholes, Nature **431**, 256 (2004); R. J. Sension, ibid. **446**, 740 (2007); G. S. Engel *et al.*, ibid. **446**, 782 (2007); H. Lee, Y.-C. Cheng, and G. R. Fleming, Science **316**, 1462 (2007).

[2] M. Mohseni, P. Rebentrost, S. Lloyd, and A. Aspuru-Guzik, J. Chem. Phys. **129**, 174106 (2008); P. Rebentrost, M. Mohseni, I. Kassal, S. Lloyd, and A. Aspuru-Guzik, New J. Phys. **11**, 033003 (2009); M. B. Plenio and S. F. Huelga, New J. Phys. **10**, 113019 (2008); F. Caruso, A. W. Chin, A. Datta, S. F. Huelga, M. B. Plenio, J. Chem. Phys. **131**, 105106 (2009); A. Olaya-Castro, C.F. Lee, F. Fassioli Olsen, and N.F. Johnson, Phys. Rev. B **78**, 085115 (2008).

[3] H.-P. Breuer and F. Petruccione, *The Theory of Open Quantum Systems*, Oxford University Press, Oxford, UK (2003); G. Lindblad, Commun. Math. Phys. **48**, 119 (1976) .

[4] W. R. Anderson, J. R. Veale, and T. F. Gallagher, Phys. Rev. Lett. **80**, 249 (1998); I. Mourachko *et al.*, ibid., 253 (1998); S. Westermann *et al.*, Eur. Phys. J. D **40**, 37 (2006).

[5] O. Mülken and A. Blumen, Physica E, in press (2009), and references therein.

[6] O. Mülken *et al.*, Phys. Rev. Lett. **99**, 090601 (2007).

[7] M. Reetz-Lamour, T. Amthor, J. Deiglmayr, and M. Weidemüller, Phys. Rev. Lett. **100**, 253001 (2008).

[8] R. Egger and C.H. Mak, Phys. Rev. B **50**, 15210 (1994); R. Egger and C.H. Mak, J. Phys. Chem. **98**, 9903 (1994).

[9] J. Gilmore and R.H. McKenzie, Chem. Phys. Lett, 421, 266 (2006).

[10] O. Mülken, V. Bierbaum, and A. Blumen, J. Chem. Phys. **124**, 124905 (2006).

[11] U. Weiss, *Quantum Dissipative Systems*, Series in Modern Condensed Matter Physics, Vol. 2 (World Scientific, Singapore, 1998).

[12] A. O. Caldeira and A. J. Leggett, Ann. Phys. **149**, 374 (1983); *ibid.* **153**, 445 (1984) [erratum].

[13] R.P. Feynman and F.L. Vernon, Ann. Phys. (N.Y.) **24**, 118 (1963).

[14] *Quantum Monte Carlo Methods in Condensed Matter Physics*, ed. by M. Suzuki (World Scientific, Singapore, 1993), and references therein.

[15] L. Mühlbacher, J. Ankerhold, and C. Escher, J. Chem. Phys. **121**, 12696 (2004); L. Mühlbacher and J. Ankerhold, J. Chem. Phys. **122**, 184715 (2005).

[16] R. Egger, C. H. Mak, and U. Weiss, J. Chem. Phys. **100**, 2651 (1994).